Available online at www.sciencedirect.com
ScienceDirect
Surface Science 602 (2008) 650–659
SURFACE SCIENCE
www.elsevier.com/locate/susc

Structure determination of PF_3 adsorption on Cu(100) using X-ray standing waves

M.S. Kariapper [a], C.J. Fisher [b], D.P. Woodruff [b,*], A.S.Y. Chan [c], Robert G. Jones [c]

[a] Department of Physics, King Fahd University of Petroleum and Minerals, Dhahran 31261, Saudi Arabia
[b] Physics Department, University of Warwick, Coventry CV4 7AL, UK
[c] Department of Physical Chemistry, School of Chemistry, University of Nottingham, Nottingham NG7 2RD, UK

Received 5 September 2007; accepted for publication 22 November 2007
Available online 8 December 2007

Abstract

The local structure of the Cu(100)$c(4 \times 2)$–PF_3 adsorption phase has been investigated through the use of normal-incidence X-ray standing waves (NIXSW), monitored by P 1s and F 1s photoemission, together with P K-edge near-edge X-ray absorption fine structure (NEXAFS). NEXAFS shows the molecule to be oriented with its C_{3v} symmetry axis essentially perpendicular to the surface, while the P NIXSW data show the molecule to be adsorbed in atop sites 2.37 ± 0.04 Å above the surface, this distance corresponding to the Cu–P nearest-neighbour distance in the absence of any surface relaxation. F NIXSW indicates a surprisingly small height difference of the P and F atoms above the surface 0.44 ± 0.06 Å, compared with the value expected for an undistorted gas-phase geometry of 0.77 Å, implying significant increases in the F–P–F bond angles. In addition, however, the F NIXSW data indicate that the molecules have a well-defined azimuthal orientation with a molecular mirror plane aligned in a ⟨011⟩ substrate mirror plane, and with a small (5–10°) tilt of the molecule in this plane such that the two symmetrically-equivalent F atoms in each molecule are tilted down towards the surface.
© 2007 Elsevier B.V. All rights reserved.

Keywords: Surface structure; Chemisorption; X-ray standing waves; Copper; Phosphorous trifluoride

1. Introduction

The chemisorption properties of phosphorous trifluoride, PF_3, have attracted significant interest due, in large part to the strong similarity as a ligand in metal coordination chemistry to that of CO, although with most transition metals it bonds only in a singly-coordinated fashion. Studies of PF_3 adsorption on extended surfaces of several metals appear to indicate similar behaviour, but have also served as model systems for the study of electron-induced dissociation and desorption phenomena. The great majority of these investigations have been on threefold symmetric substrates: Pd(111) [1], Ni(111) [1–4], Pt(111) [5], Ru(0001) [6], Cu(111) [7], and in the case of Ni(111) and Cu(111) quantitative structure determination (mainly based on normal-incidence X-ray standing waves (NIXSW) [3,7] and scanned-energy mode photoelectron diffraction (PhD) [4]) have shown the bonding to be to singly-coordinated atop sites, with the molecular C_{3v} symmetry axis essentially perpendicular to the surface. One interesting aspect of the adsorption of PF_3 on these surfaces is the extent to which the adsorbed molecules are azimuthally aligned, or are freely rotating about their C_{3v} symmetry axis. On both Ni(111) [2] and Ru(0001) [6] it has been shown, using ESDIAD (electron-stimulated desorption ion angular distributions), that at low coverages (~0.04 ML) azimuthal alignment occurs only at low temperatures (typically ~80 K or less), but at saturation coverages of 0.25 ML or 0.33 ML, free rotation is suppressed even at room temperature. This latter finding is broadly consistent with the fact that the intermolecular distances in these high-coverage ordered phases (4.97 Å and

* Corresponding author. Tel.: +44 2476523378; fax: +44 2476692016.
E-mail address: d.p.woodruff@warwick.ac.uk (D.P. Woodruff).

0039-6028/$ - see front matter © 2007 Elsevier B.V. All rights reserved.
doi:10.1016/j.susc.2007.11.025

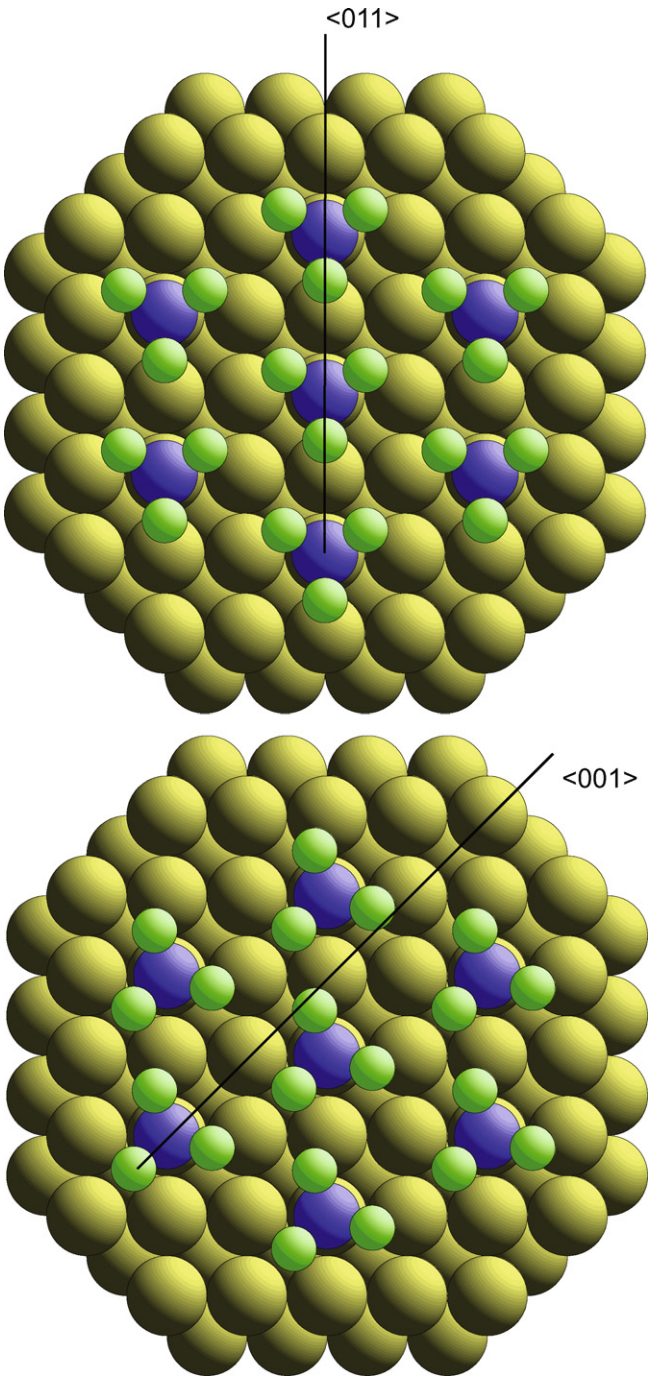

Fig. 1. Schematic diagram of the Cu(100)$c(4 \times 2)$–PF_3 surface phase assuming the molecules are located in atop sites (as found in the present study). The structure is shown for two possible azimuthal orientations of the molecule corresponding to alignment of a molecular mirror plane with one of the two inequivalent mirror planes of the substrate.

4.68 Å, respectively) are significantly smaller than the estimated van der Waals diameter (relative to the symmetry axis and thus parallel to the surface) of about 5.4 Å [1], leading to steric hindrance of the rotational movement. There has also been some interest in the vibrational motion of the adsorbed PF_3 molecules relative to the surface, the atop adsorption site tending to favour large-amplitude frustrated translational motion parallel to the surface, first noted in NIXSW experiments on Ni(111) [3].

Somewhat more recently Braun et al. [8] have investigated the properties of PF_3 adsorption on a fourfold symmetric surface, that of Cu(100), using, in particular, elastic and inelastic helium atom scattering. Their results show the formation of a $c(4 \times 2)$ ordered phase at a nominal coverage of 0.25 ML (see Fig. 1) for which the nearest- and next-nearest intermolecular distances are 5.11 Å and 5.71 Å, values that may, or may not, be sufficiently short to allow azimuthal rotation of the adsorbed molecules. This study also provided clear evidence of a frustrated translational surface vibration, and also identified a higher coverage incommensurate phase at low temperature that, by implication, must involve at least some molecular adsorption in multiply-coordinated sites.

Here, we present the results of an experimental investigation of the Cu(100)$c(4 \times 2)$–PF_3 surface phase using NIXSW and NEXAFS (near-edge X-ray absorption fine structure). NIXSW [9,10] involves the measurement of the element-specific X-ray absorption, in the present case by monitoring the P 1s and F 1s photoemission signal, in an X-ray standing wavefield established due to the interference of the incident and scattered X-rays at a Bragg reflection in the crystalline sample. By monitoring the absorption profile as the photon energy is scanned through the Bragg condition, leading to a systematic shift in the location of the standing wavefield, the location of the absorbing atoms relative to the substrate scatterer atoms can be determined. Complementary information on the adsorbed molecular orientation is provided by the polarisation-angle dependence of the NEXAFS signal. Together these methods allow us to determine the local adsorption geometry, and specifically, the adsorption site, and to explore the evidence for azimuthal ordering.

2. Experimental details

The experiments were conducted in a purpose-built UHV surface science end-station taking radiation from a double-crystal monochromator (station 6.3) installed on the SRS (synchrotron radiation source) at the CCLRC Daresbury Laboratory. The NEXAFS spectra and the NIXSW absorption profiles were obtained by measuring the intensity of an element-specific Auger or photoelectron emission peak using a concentric hemispherical electron-energy analyser (VSW Ltd.) mounted in the horizontal plane at a fixed angle of 40° to the incident synchrotron radiation. The Cu(100) sample was prepared by the usual combination of X-ray Laue orientation, spark machining, mechanical polishing, and in situ argon ion bombardment and annealing cycles until a clean well-ordered surface was obtained as indicated by Auger electron spectroscopy (AES) and low energy electron diffraction (LEED). Adsorbate dosing of the surface was effected by exposing the sample at a temperature of 110 K to PF_3 gas introduced into the chamber to a typical pressure of 5×10^{-8} mbar.

An exposure of 2×10^{-6} mbar s appeared to be sufficient to ensure saturation coverage within a single layer; higher exposures led to no further adsorption and no formation of multilayers. The sample was then briefly annealed to 180 K to ensure that only the $c(4 \times 2)$ phase was present on the surface and not the higher-coverage incommensurate phase found by Braun et al. [8] for temperatures below 145 K. Adsorbed PF_3 is known to have a high cross-section for electron beam desorption and dissociation (e.g. [7,8,11–13]), so LEED and AES data recorded from the adsorbate surface (to check for contaminants such as oxygen and carbon) were carried out only after the NIXSW or NEXAFS measurements had been completed. These checks with LEED did reveal the expected $c(4 \times 2)$ diffraction pattern, but this was only seen for a few seconds before being replaced by a (1×1) structure, clear evidence of this radiation damage. Incident photons can also cause fragmentation (probably by an electron-mediated process) of adsorbed PF_3, leading to characteristic chemical shifts in the P 2p and 1s photoemission spectra associated with the PF_x fragments (e.g. [13,14,15]), but careful checks of the P 1s and F 1s photoemission spectra before and after the NIXSW measurements (which typically took ~3 h) showed no such effects; this lack of damage may be attributed to the use of a low incident flux-density of relatively poorly-focussed bending-magnet synchrotron radiation.

For the NIXSW measurements, X-ray absorption in the copper substrate was monitored by the intensity of the Cu L_3VV Auger transition (920 eV). The absorption at the F and P atoms was obtained by monitoring the intensities of the F 1s photoemission (697 eV binding energy) and P 1s photoemission (2146 eV binding energy) signals. In most cases these intensities were taken as the difference between the electron emission at the peak energy and the intensity measured at a kinetic energy a few eV higher. In the case of the NIXSW experiment from the (1 1 1) scatterer planes (Bragg energy ~2975 eV), however, a different approach (previously described by Jones et al. [7]) was necessary to monitor the X-ray absorption at the P atom. This is because, over the range of the photon energy used, the P 1s photoemission peak crosses the Cu $L_3M_{2,3}V$ Auger peak, at 840–849 eV kinetic energy, on the high photon energy side of the standing wave condition. In order to achieve effective separation of the intensity contributions from these two peaks, a wide range energy distribution curve (EDC) of the Cu Auger peak was recorded using a photon energy set to a value ~170 eV below the Bragg energy, chosen so that the P 1s peak is not present in this range. This EDC (after normalisation to the X-ray beam flux) was then used as the standard structured background spectrum. A series of narrow EDCs of the P 1s peak for a set of photon energies across the standing wave condition was then obtained and each normalised to the X-ray beam flux. The standard background spectrum was then matched to the high kinetic energy end of these individual P 1s EDCs by a multiplication factor, and subtracted from the narrow EDC, leaving just the P 1s photoelectron peak. The P 1s spectra obtained in this way were fitted using a Doniac-Sunjic line shape [16], and the peak heights were extracted to form the absorption curve for phosphorus. The fitting factors used in this background subtraction procedure reproduce the fluctuations in the copper substrate background emission intensity through the standing wave scan, and can be used as a measure of the NIXSW absorption signal in the copper substrate.

Phosphorous K-edge NEXAFS data were obtained by monitoring the P KLL Auger peak intensity (KE 1859 eV) as the X-ray energy was scanned through the P K-edge (2146 eV). Spectra were recorded in five different incidence angles; using the standard NEXAFS nomenclature of the grazing incidence angle (the angle between the photon beam and the surface plane), these were 90° (normal incidence) 60°, 45°, 30° and 15°.

3. Results and structural analysis

3.1. NEXAFS

The P K-edge NEXAFS spectra are shown in Fig. 2. Individual spectra are normalised to the incident X-ray beam and then all five spectra were normalised to a constant edge jump (far above the edge), to match around the first EXAFS oscillation at ~2165 eV. This is considered an adequate procedure as variations in the intensities of the EXAFS oscillations with detection angle are expected to be

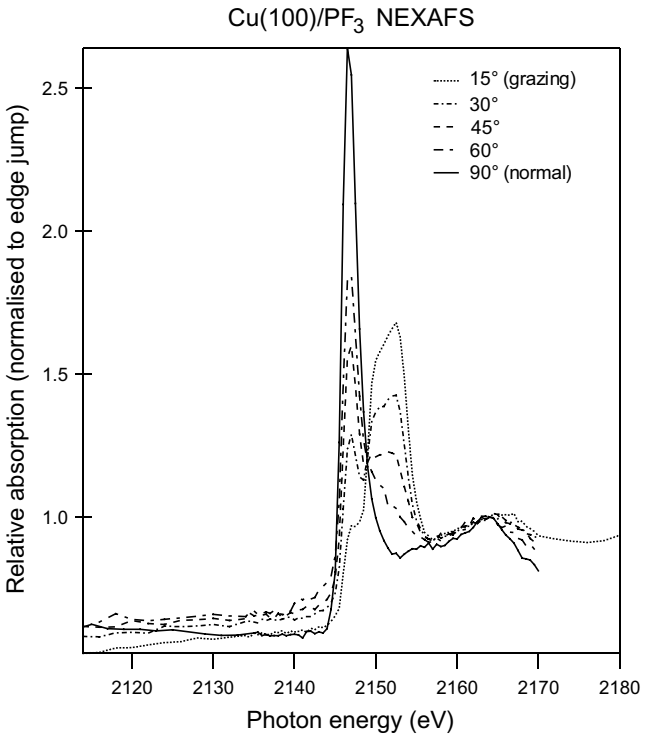

Fig. 2. P K-edge NEXAFS spectra from the Cu(100)$c(4 \times 2)$–PF_3 surface recorded at five different incidence angles. Note that no absolute calibration of the photon energy scale was conducted in these experiments, as only the relative energies are significant for this investigation.

small compared to the variations in the NEXAFS peak intensities, which are our primary concern here.

Two clearly-resolved NEXAFS peaks, at ~2146.5 eV and ~2152.5 eV, are seen. When the sample is moved towards normal incidence the first peak grows in intensity and the second peak disappears, whereas at grazing incidence the second peak grows and the first peak fades. As described in Ref. [7] for the same molecule adsorbed on Cu(1 1 1), the lower energy peak is associated with a transition from the fully symmetric P 1s state into the lowest unoccupied π-symmetry (strictly e-symmetry) 7e orbital of the molecule, partially occupied by π back donation from the metallic d orbitals, whilst the second peak corresponds to the transition to the σ-symmetry $8a_1$ orbital of molecule. In fact, inspection of Fig. 2 indicates that the σ-resonance peak consists of two components with identical or closely similar dependence on the polarisation direction. Why this should be in unclear; a tilt of the molecule on the surface could lead to a splitting of the π-state due to loss of degeneracy of the π_x and π_y state, but there should be no equivalent effect on the σ-state. However, we make no explicit use of the σ-resonance peak, and so do not consider this problem further. The degree of polarisation of the synchrotron radiation at these energies is 90%, with the electric vector in the plane of the incidence, and this means that at normal incidence the electric vector is parallel to the crystal surface, whereas at 0° grazing incidence it would be perpendicular to the surface. Therefore the absence of the a_1 peak at normal incidence and the large drop in intensity of the e-symmetry peak on going to grazing incidence shows that the C_{3v} axis of the molecule is aligned perpendicular to the surface. No detailed quantitative analysis of these peak intensities has been undertaken, but it is clear that the near-edge π-resonance at grazing incidence is either extremely small or of essentially zero intensity depending on the position of the continuum edge-jump. As such, we conclude that the molecule has this perpendicular orientation to within a typical NEXAFS precision of ±10° (e.g. [17]).

3.2. NIXSW

The NIXSW absorption profiles monitored from the P 1s and F 1s photoemission signals through the (2 0 0) and (1 1 1) reflection conditions are shown in Fig. 3. These experimental NIXSW profiles were analysed using the XSWfit automated fitting procedure [18]. NIXSW analysis provides two structural parameters [9,10,19]: the coherent position d_H (where H specifies the Miller indices of the scatterer planes) and the coherent fraction f_{co}. In the simplest case of an absorber occupying a single well-defined site, d_H is equal to the perpendicular distance of this site from the scattering planes, while f_{co} is a measure of the degree of local order. Notice that d_H is defined relative to the nearest extended scatterer plane, so even in this simplest structural situation the real distance may differ from the coherent position by an integral number of substrate inter-

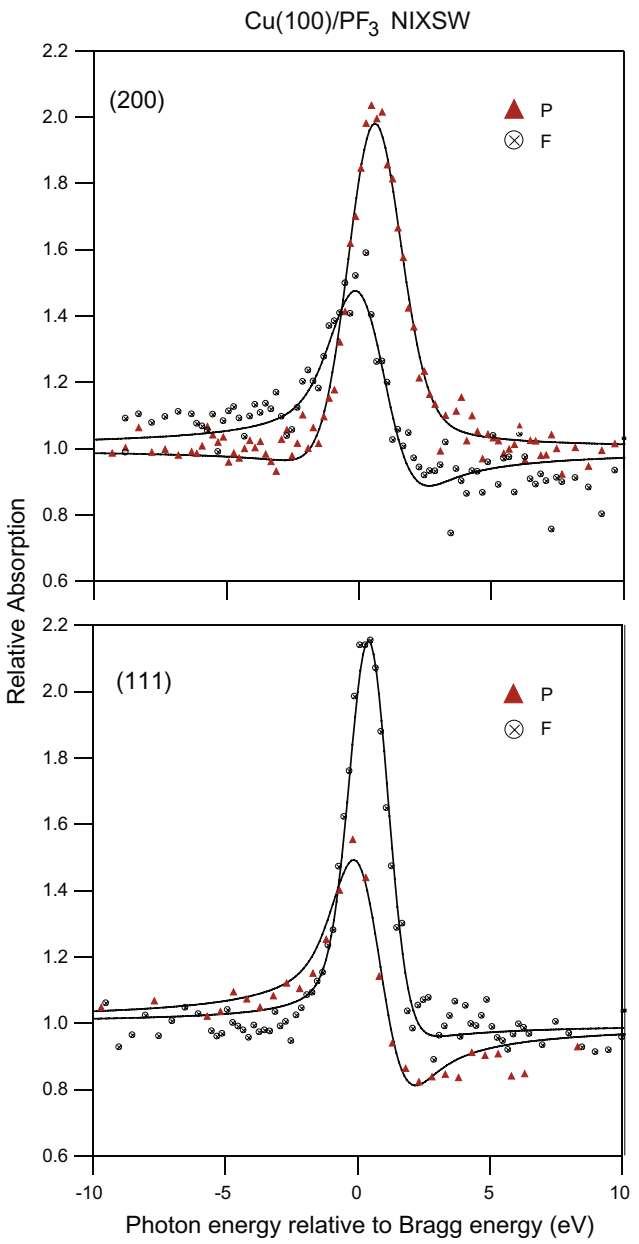

Fig. 3. Experimental NIXSW (2 0 0) and (1 1 1) absorption profiles (symbols) from the P and F absorbers together with best-fit theoretical curves using the structural parameter values listed in Table 1. Reduced photon energy steps were used in the data collection in the most structure-sensitive range at energies close to the nominal Bragg energy.

layer spacings. More generally, f_{co} can only take values between 0 and 1; some reduction below the ideal value of 1 for a single well-defined site to ~0.8–0.9 arises from dynamic (thermal vibrations) and static local disorder. Much lower values can occur, but this generally implies that there is multiple site occupation. The shape of the profiles is also influenced by two non-structural parameters, the Gaussian instrumental broadening ΔE (mainly due to the finite resolution of the monochromator) and the absolute energy of the Bragg reflection E_B. These parameters were determined by fitting the substrate standing wave profile, and were

then fixed for the analysis of the adsorbate absorption profiles, which were then fitted by only adjusting the adsorbate structural parameters.

For a more general understanding of the relationship between the XSW structural parameters of the coherent position and coherent fraction, and the actual positions of absorber atoms, a rather more formal discussion is required. In particular, to analyse situations involving two or more distinct absorber sites one exploits the finding that the coherent fraction and coherent position can be related to the spatial distribution of the absorber atoms relative to the nearest scatterer plane $f(z)$, defined by the spacing coordinate z, by

$$f_{co}\exp(2\pi i d_H/D_H) = \int_0^{D_H} f(z)\exp(2\pi i z/D_H)\mathrm{d}z \qquad (1)$$

where D_H is the bulk interlayer spacing of the H scatterer planes [2–4]. From this it is clear that f_{co} and d_H/D_H define the amplitude and phase of one Fourier component of the absorber site distribution projected along one direction (perpendicular to the relevant Bragg scatterer planes). Notice that the left-hand side of this equation can be represented as a vector in an Argand diagram with length f_{co} and direction determined by the phase angle $2\pi d_H/D_H$ relative to the positive real axis [20]. The right-hand side of the equation is then a summation (integral) over component vectors of length $f(z)$ and phase angle $2\pi z/D_H$. This interpretation is particularly useful in summing over discrete sites at spacings z_i, in which case $f(z)$ is replaced by a set of discrete occupation probabilities, p_i, leading to

$$f_{co}\exp(2\pi i d_H/D_H) = \sum_i p_i \exp(2\pi i z_i/D_H)\mathrm{d}z \qquad (2)$$

The NIXSW structural parameter values obtained from the data of Fig. 3 are summarised in Table 1, while the quality of the resulting fits to the experimental data are shown in Fig. 3. These functional fits, both based on monitoring 1s photoemission signals, include the effects of non-dipole effects in the angular dependence of the photoemission, leading to a forward/backward asymmetry parameter Q, and to a small offset in the coherent position due to a phase factor introduced by these non-dipole effects. The values of these correction terms have been determined in previous calibration experiments for the Cu(111) and (200) NIXSW energies [21]; specifically Q values for the (111) and (200) conditions used were, respectively, 0.18 and 0.25 for P 1s, and 0.25 and 0.31 for F 1s. Note that the error estimates in Table 1 are based on the scatter of several different experimental measurements; error estimates based on the least-squares fitting to individual data sets are actually significantly smaller.

In order to interpret these structural parameters in terms of the actual structure, we consider first the P atom which we expect to be bonded to the surface in a single atomic site. In this context we note that the value of $f_{(200)}$ is quite close to unity, reinforcing the view that all P atoms have essentially the same height above the surface. The (200) coherent position provides information on the height of the P atom above the Cu(100) surface, but because the XSW measurement provides the distance of the atoms from the nearest extended substrate scatterer plane, the true height above the outermost Cu atom layer is $z_{(200)} = d_{(200)} + nD_{(200)}$, where n is an integer. In principle, n could take any integral value, but in practice only one value is likely to lead to a plausible Cu–P nearest-neighbour distance. Notice, though, that if the outermost interlayer spacings of the Cu(100) surface are relaxed, the net relaxation will constitute a systematic error between $z_{(200)}$ as determined by this equation, and the true nearest-neighbour Cu–P interlayer spacing. In practice, it is highly improbable that this net relaxation (i.e. the relaxation integrated over all relaxed layers, which typically have alternating sign with layer thickness) is greater than 0.1 Å, and is almost certainly much less than this, so this problem has a minimal impact on the proper choice of n.

Table 2 shows the Cu–P nearest-neighbour distances (assuming no net relaxation) for n values of 0 and 1 for each of the three highest-symmetry adsorption sites,

Table 1
Summary of NIXSW structural parameters obtained from absorption at the P and F atoms of PF_3 adsorbed on Cu(100)

Parameter/absorber	$d_{(200)}$ ($d_{(200)}/D_{(200)}$)	$f_{(200)}$	$d_{(111)}$ ($d_{(111)}/D_{(111)}$)	$f_{(111)}$
P	0.56 ± 0.04 Å (0.31 ± 0.02)	0.89 ± 0.045	1.35 ± 0.04 Å (0.65 ± 0.02)	0.69 ± 0.05
F	1.00 ± 0.04 Å (0.55 ± 0.02)	0.66 ± 0.05	0.77 ± 0.04 Å (0.36 ± 0.02)	0.43 ± 0.05

The coherent positions are shown both in the form of d_H (in Ångström units) and of d_H/D_H (a dimensionless quantity), the latter shown in brackets.

Table 2
Implications of specific P adsorption sites compatible with the measured NIXSW $d_{(200)}$ value and the predicted $d_{(111)}$ values

Adsorption site	Cu–P nn distance with $z_{Cu-P} = d_{(200)}$	Predicted $d_{(111)}$ value with $z_{Cu-P} = d_{(200)}$	Cu–P nn distance with $z_{Cu-P} = d_{(200)} + D_{(200)}$	Predicted $d_{(111)}$ value with $z_{Cu-P} = d_{(200)} + D_{(200)}$
Atop	0.56 ± 0.04 Å	0.32 ± 0.02 Å	*2.37 ± 0.04 Å*	*1.36 ± 0.01 Å*
Hollow	1.89 ± 0.01 Å	1.36 ± 0.01 Å	2.98 ± 0.03 Å	0.32 ± 0.02 Å
Bridge	1.39 ± 0.02 Å	Indeterminate ($f_{(111)} = 0$)	2.69 ± 0.04 Å	Indeterminate ($f_{(111)} = 0$)

The values shown in italics are those corresponding to the solution consistent with NIXSW triangulation and bond length considerations, as described in the text.

namely onefold coordinated atop, fourfold coordinated hollow, and twofold coordinated bridge sites. A NIXSW study of PF_3 adsorption on Cu(1 1 1) [7] inferred a value of the Cu–P distance of 2.25 ± 0.04 Å, so we may expect a value on Cu(1 0 0) within about 0.1 Å of this value. The only structure in Table 2 to satisfy this constraint corresponds to atop adsorption with a value of n of 1, and thus a value of $z_{(200)}$ of 2.37 ± 0.04 Å. Valuable additional information in making this selection, and even more significantly to determine the adsorption site, is provided by the (1 1 1) coherent position. In particular, for a specific height of the absorber atom above the surface, $z_{(200)}$, we can predict the value of $d(1\,1\,1)$ to be expected for different adsorption sites by simple triangulation. Specifically, for the two fully-symmetric sites (the sites that retain the full point group symmetry of the substrate), the general relationships are:

$$\text{atop} : z_{(111)} = z_{(200)} \sin 35.26^\circ = z_{(200)}/\sqrt{3} \tag{3a}$$

$$\text{hollow} : z_{(111)} = (z_{(200)} + D_{(200)}) \sin 35.26^\circ = 0.5D_{(111)} + (z_{(200)}/\sqrt{3}) \tag{3b}$$

These predicted values are included in Table 2, which shows that the atop geometry (with $n = 1$) would be expected to yield a $d_{(111)}$ value almost identical to the measured value. Notice that Table 2 also shows that, on the basis of the triangulation of the (2 0 0) and (1 1 1) XSW parameters alone, there is an ambiguity between the atop site with $n = 1$, and the hollow site with $n = 0$. This is because both sites correspond to the P atom lying at the same height atop a Cu atom, in one case atop a first layer atom, in the other case atop a second layer atom. The XSW technique does not distinguish these situations, but the different implied Cu–P nearest-neighbour distances clearly allows us to reject the hollow site model.

Table 2 also shows that it is straightforward to reject the possibility of bridge site adsorption, even without considering the bond lengths, because the predicted (1 1 1) coherent fraction value for these sites is identically zero. Because the bridge sites have only twofold rotational symmetry on a fourfold symmetric substrate, there are two inequivalent bridge sites (related by a 90° azimuthal rotation) that must have equal occupation. The $d_{(111)}$ values for these two sites (that are the same as for the atop and hollow sites, respectively) differ by $D_{(111)}/2$, leading to a net cancellation and the zero value of $f_{(111)}$, as may be recognised by substitution of this two-state solution into Eq. (2) with $p_1 = p_2 = 0.5$ and $z_2 = z_1 + 0.5D_{(111)}$.

The clear conclusion that the PF_3 molecule adsorbs in a onefold coordinated atop site on Cu(1 0 0) is, of course, consistent with our expectations of the general chemistry of this species. One further feature of the NIXSW data that is qualitatively consistent with this conclusion is the fact that for the P atoms the value of $f_{(111)}$ is significantly lower than that of $f_{(200)}$. In studies of a range of molecular adsorbates on surfaces, using both NIXSW and photoelectron diffraction, we have found evidence for atop-bonded species to show large-amplitude wagging vibrational modes corresponding to frustrated rotation, with most of the motion parallel to the surface. In NIXSW such motion has little effect on the coherent fraction measured for standing wave nodal planes parallel to the surface, as the height variation is small, but leads to a marked reduction of the coherent fraction for measurements with nodal planes steeply inclined relative to the surface. For example, this effect was seen in a NIXSW study of PF_3 adsorbed (in atop sites) on Ni(1 1 1) using the (1 1 1) (scatterer planes parallel to the surface) and $(\bar{1}\,1\,1)$ (scatterer planes inclined at 70° to the surface), for which the P coherent fraction values were 0.8 and 0.5, respectively, attributed to a root-mean-square (rms) vibrational amplitude parallel to the surface of approximately 0.27 Å [3]. The reduction of the coherent fraction between the (2 0 0) and (1 1 1) NIXSW in the present case could be reconciled with a very similar value of the rms vibrational amplitude. Of course, an alternative source of this reduced $f_{(111)}$ value could be a *static* rather than dynamic offset of the P atom from the exact atop site by a similar amount, implying a tilt of the Cu–P bond relative to the surface normal.

For further information on the adsorption geometry we now turn to the F (2 0 0) NIXSW structural parameter values of Table 1. As for the P atom, the only plausible value of $z_{(200)}$ corresponds to adding one bulk interlayer spacing to the measured $d_{(200)}$, leading to a value 2.81 Å, just 0.44 Å higher above the surface than the P atoms. This small difference in height of the P and F atoms is surprising. In the gas-phase molecule the P–F distance projected onto the C_{3v} symmetry axis is 0.77 Å, and the NIXSW studies of PF_3 adsorbed on Ni(1 1 1) [3] and Cu(1 1 1) [7] the height difference of the P and F atoms above the surface was found to be 0.75 ± 0.15 Å and 0.80 ± 0.06 Å, respectively, both consistent with adsorption of an undistorted molecule adsorbed with the molecular C_{3v} axis perpendicular to the surface. In the present case the much smaller interlayer spacing of the P and F atoms clearly implies a substantial increase in the F–P–F bond angles relative to the gas-phase molecule if the molecular symmetry axis is perpendicular to the surface. A tilt of this axis, however, could partially account for the reduction in the average P–F interlayer spacing relative to the surface normal. Of course, tilting the PF_3 axis leads to some F atoms moving down and others moving up, but if the tilt plane corresponds to a mirror plane of the molecule such that two F atoms move down and one moves up, the weighted average height, as monitored by the coherent position, is reduced. Such a difference in height of the F atoms relative to the surface could also account for the fact that $f_{(200)}$ for the F atoms is significantly lower than the value for the P atoms.

In order to explore this idea a little further a simple calculation was undertaken of the (2 0 0) F coherent position and coherent fraction, as a function of the tilt angle of the C_{3v} molecular symmetry axis, and of the F–P–F angle, assuming the P–F bond length is fixed at the gas-phase value of 1.57 Å and the difference in the P and F coherent

positions is 0.44 Å, as measured. A solution was found with a tilt angle of 13°, but this solution also retains the large F–P–F bond angle distortion, the projection of the P–F bond along the molecular symmetry axis being 0.47 Å, only slightly larger than the difference in the $d_{(200)}$ values. Nevertheless, it is notable that such a tilt angle would place the P atoms 0.53 Å off atop, leading to a 40% reduction in $f_{(111)}$ relative to $f_{(200)}$ (see Fig. 4 discussed below). This is a significantly larger effect than that seen in the experimental data, so while a small tilt may help to reconcile some aspects of the (200) coherent fractions, other sources of disorder must contribute. Significantly, the much-reduced P–F spacing along the molecular symmetry axis is not significantly changed by incorporating tilting, so this effect seems to be an inescapable implication of the experimental data.

We finally turn to the (111) NIXSW parameter values for the F atoms; can this information provide any specific information on the lateral positions of the F atoms and thus the azimuthal alignment of the adsorbate PF_3 species? The fact that $f_{(111)}$ is very significantly larger than zero suggests that some such information should be available. Of course, for any location of the threefold symmetric PF_3 molecule on the fourfold symmetric Cu(100) surface, at least some of the F atoms must be in low symmetry sites relative to the substrate, so we need to understand how

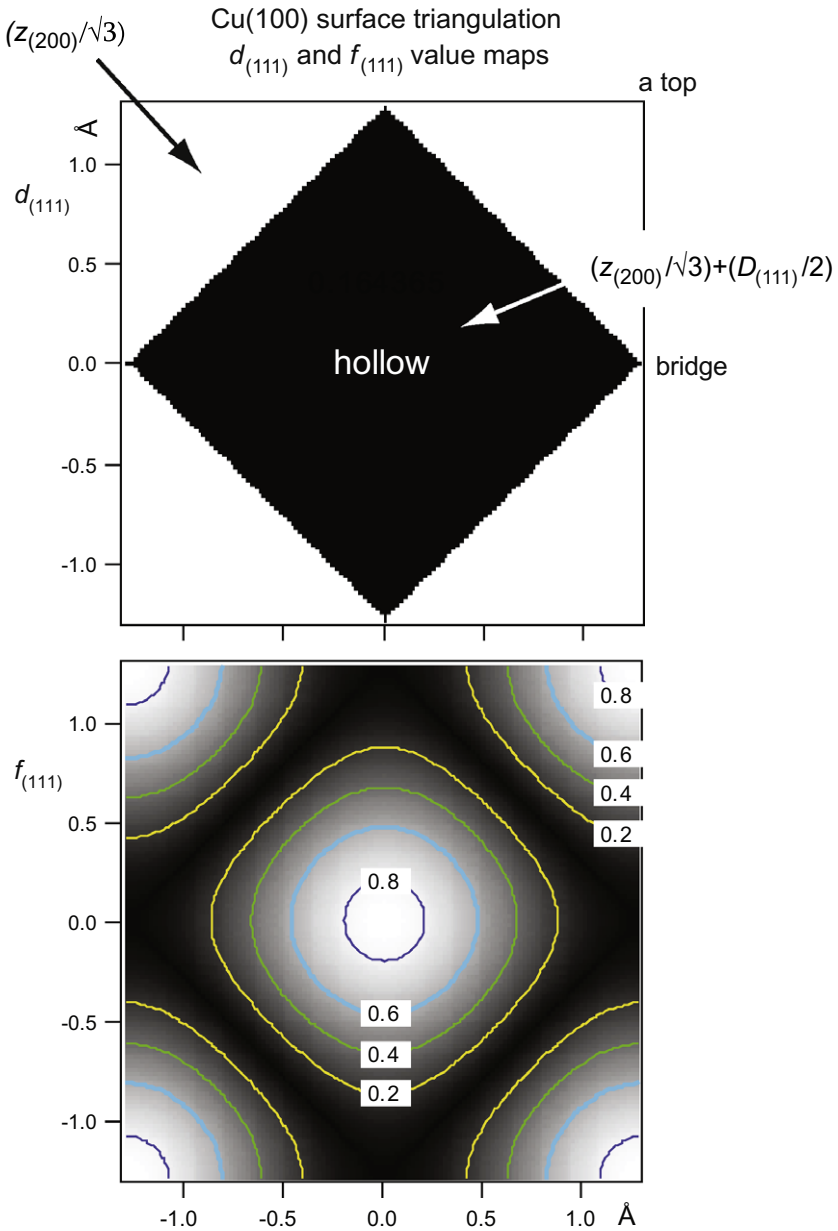

Fig. 4. Grey-scale-shaded contour maps, as a function of lateral position on a Cu(100) surface, of the values of the NIXSW parameters, $d_{(111)}$ and $f_{(111)}$, for a single absorber atom at a height $z_{(200)}$ above the surface.

the (200) and (111) XSW structural parameters triangulate for low symmetry adsorption sites. This can be established through the use of Eq. (2) above, where the summation is over all symmetrically equivalent sites on the surface (related by the point group symmetry operations of the substrate). The results, for photo-absorption at a single adsorbed atom in all possible lateral positions on the surface, are given in Fig. 4, which shows grey-scale-shaded contour maps of the values of $d_{(111)}$ and $f_{(111)}$ within a surface unit mesh. A striking result is that there are only two possible values of $d_{(111)}$ for a specific height of the absorbed atom above the surface, $z_{(200)}$. These specific values correspond to those associated with the high-symmetry atop and hollow sites given in Eq. (3) above, so the map in $d_{(111)}$ shows only the two extreme grey levels, black and white. The map in $f_{(111)}$ shows how the sudden switches between these two discrete $d_{(111)}$ can occur, because the coherent fraction goes to zero at the boundary between these two distinct values of $d_{(111)}$. Moreover, the value of this coherent fraction, that is unity at the two four-fold symmetric atop and hollow sites, falls smoothly as the adsorption site is displaced further and further from these high-symmetry locations. Thus, within an Argand diagram representation, the vector representing the solution becomes shorter and shorter (decreasing $f_{(111)}$) as one moves off the high-symmetry sites, and switches direction (and thus $d_{(111)}$ value) as its length passes through zero.

Of course, in the present case, we have three F atoms per adsorbed molecule, constrained in their relative positions by the intramolecular bonding, so simple symmetry arguments (the only common symmetry property that the surface and molecule can share is a mirror plane) show that there must be at least two symmetrically-distinct F atom sites on the surface. Notice, though, that the only two possible $d_{(111)}$ values differ by $D_{(111)}/2$, so their associated Argand vectors are diametrically opposed. Any mixture of surface sites must therefore lead to a summation involving these two discrete values, weighted according to the location of the contributing sites. Thus, if we sum components having these two values with the same occupancy (as in the bridge site discussed above), then the coherent fraction is zero (the vectors cancel). If their occupancies are different, the resultant vector has the direction (coherent position) of the higher-occupancy component, but a much reduced amplitude due to the partial cancellation. We therefore conclude that, not only does any single adsorption site on this fcc(100) surface lead to only two possible values, of $d_{(111)}$, but *any combination of surface sites* also can lead to only one of these two values.

Turning now to the experimental data, if we take $z_{(200)}$ for the F atoms to be 2.81 ± 0.04 Å as discussed above, then the two possible $d_{(111)}$ are 1.62 ± 0.02 Å (atop) and 0.72 ± 0.02 Å (hollow). The experimental value is 0.77 ± 0.04 Å, clearly consistent with the hollow-site value. To understand the implications of this result, and the potential significance of the measured value of $f_{(111)}$, Fig. 5 shows the triangulation maps of Fig. 4 re-plotted over 4 unit meshes of the clean surface, each map having a (yellow[1]) circle superimposed around the P atop site at a radius of 1.5 Å. This circle corresponds to all possible locations of the F atoms, assuming an untilted species, a P–F bond length of 1.57 Å, and the distorted molecular F–P–F angle consistent with the measured value of the P–F distance projected along the molecular symmetry axis of 0.44 Å. Also superimposed on these plots are two specific azimuthal orientations of the P–F bonds (shown as dashed (yellow[1]) and solid (green[1]) lines) corresponding to one of the mirror planes of the molecule being aligned to one of the mirror planes of the substrate, as shown in Fig. 1. Notice that almost all points on the circle defining possible F

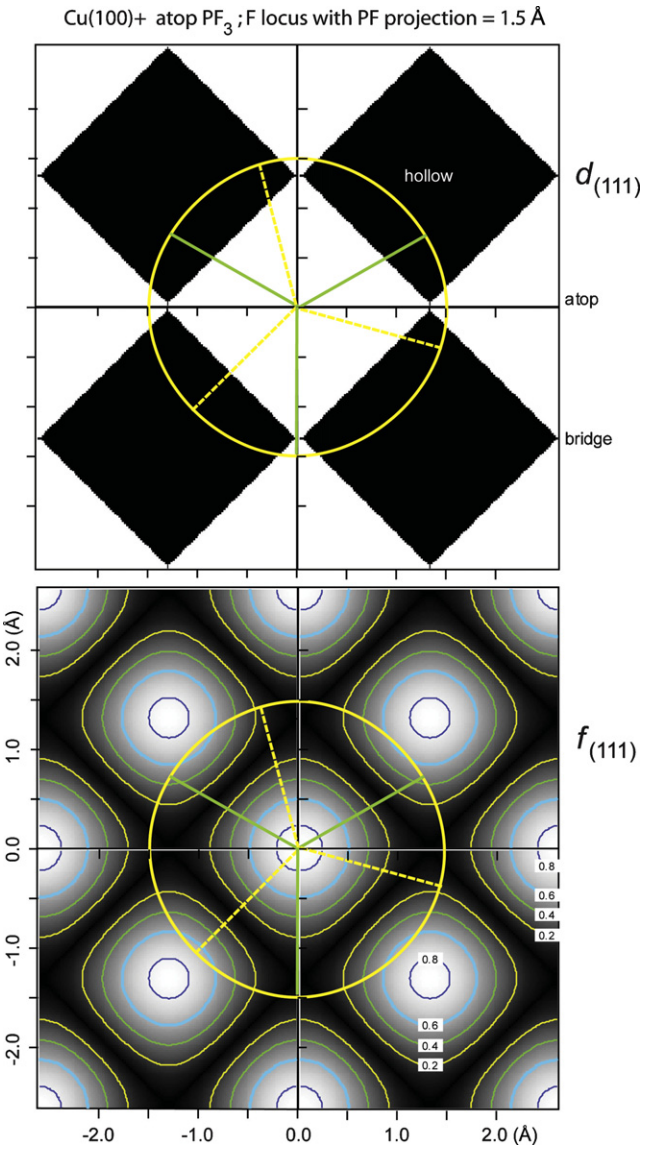

Fig. 5. NIXSW contour maps as shown in Fig. 4, but over an area of four Cu(100) surface meshes, including a superimposed locus of possible F atoms sites for atop PF_3 as found in this study.

[1] For interpretation of the references to colour in the text, the reader is referred to the web version of this article.

locations lie within the region of hollow-site $d_{(111)}$ values, so the experimental result is entirely consistent with this picture.

The points of intersection of the P–F bonds with the circle on the $f_{(111)}$ map provide a route to estimate the expected (1 1 1) coherent fraction to be measured for the two specific azimuthal orientations shown in Fig. 1. With the ⟨0 0 1⟩ mirror plane alignment, corresponding to the (yellow[1]) dashed P–F bond projections, all three F atoms lie in the regions of hollow-site triangulation, one falling on a $f_{(111)}$ contour corresponding to a value of ~0.65, the other two with $f_{(111)}$ values of ~0.15. The experimental $f_{(111)}$ value to be expected is thus the weighted average of these, namely $(0.65 + 0.15 + 0.15)/3 = 0.32$. For alignment in the ⟨0 1 1⟩ mirror plane, represented by the (green) solid P–F bond projections, two F atoms are in equivalent sites with hollow site $d_{(111)}$ values and individual $f_{(111)}$ values of ~0.47, while the third F atom is in a region (close to a bridge site) corresponding to atop-site triangulation but with a very small $f_{(111)}$ value of ~0.05. In this case, therefore, the weighted average coherent fraction expected is $(0.47 + 0.47 - 0.05)/3 = 0.30$. Bearing in mind the experimental precision, these two predicted (1 1 1) coherent fraction values are thus indistinguishable, and indeed, it is clear that from inspection of Fig. 5 that a random azimuthal orientation (or a freely rotating molecule) would give essentially the same value.

Comparison with experiment, however, indicates that the true value of the (1 1 1) coherent fraction is larger than these predicted values. The measured value is 0.43, but this value must also include the consequences of whatever disorder or tilt leads to the experimental value of $f_{(200)}$ (0.66) that is significantly reduced from the ideal value of unity. In considering this substantial reduction of $f_{(200)}$ in our discussion above, we concluded that one model that could account for this, at least in part, was if the molecule was tilted within its mirror plane such that two F atoms are lower above the surface than the third F atom. In the case of alignment in the ⟨0 1 1⟩ substrate azimuth, the consequence of such a tilt can be estimated by displacing the F-locus circles upwards in Fig. 5. This will clearly have the effect of significantly increasing the $f_{(111)}$ values of the two F atoms in the upper half of the figure maps, as these atoms move closer to the symmetric hollow sites, while the effect on the $f_{(111)}$ value of the third F atom will be minimal as this passes through a bridge site with zero coherent fraction. Such a tilt thus markedly improves the fit to the measured $f_{(111)}$ value, as well as the $f_{(200)}$ value, for the F atoms. Notice that quite a small tilt angle will have a large effect – a tilt of 10° produces a shift in the circle (which becomes very slightly ellipsoidal) on the contour maps of Fig. 5 by almost 0.5 Å, sufficient to place the two F atoms in the upper half of the figure very close to the symmetric hollow sites. By contrast, for the alignment of the molecular mirror plane in the ⟨0 0 1⟩ azimuth, tilting has the opposite effect. In this case the circle is displaced towards the top right-hand corner of the figure, and the individual $f_{(111)}$ values of all the contributing F atoms are reduced.

Notice that these arguments relate to a static tilt of the molecular axis. The reduced $f_{(111)}$ value for the P absorbers could be attributed to either dynamic time-averaged tilt of the molecular axis, or a static tilt (averaged over symmetrically equivalent domains). The same is not true in attempting to understand the $f_{(111)}$ value for the F absorbers, which is actually *higher* than would be expected for a rigid perpendicularly-aligned molecule. In particular, this increase in the coherent fraction is associated with a particular sign of the tilt in a particular azimuthal direction; tilting in the opposite sense would lead to a reduced value of $f_{(111)}$, so a wagging motion symmetric about the surface normal will not have the same effect as the static tilt.

4. General discussion and conclusions

The NIXSW data presented here clearly show that the PF_3 species in the Cu(1 0 0)$c(4 \times 2)$–PF_3 surface phase are adsorbed in onefold coordinated atop sites, the triangulation of both the P and F atom coherent fractions supporting this interpretation, with the molecular C_{3v} axis at least approximately perpendicular to the surface. This result is consistent with all other quantitative structure determinations for PF_3 adsorbed on surfaces, and with the known behaviour of PF_3 as a ligand in coordination chemistry. The P K-edge NEXAFS data also clearly support this molecular orientation, although these data do not exclude the possibility of a small (~10°) static or dynamic tilting of the molecular axis. The reduced value of the NIXSW (1 1 1) coherent fraction for the P absorbing atoms could be due to a substantial amplitude of atomic vibrations parallel to the surface, consistent with a similar conclusion for PF_3 adsorbed on Ni(1 1 1) [3], and with the observation of a frustrated translational mode in an inelastic helium scattering investigation [8] of the same surface phase on Cu(1 0 0) investigated here. However, this reduced P coherent fraction could also be due to a static, rather than dynamic, lateral offset of the P atoms from the exact atop site that would accompany a molecular tilt. In this regard it is notable that more detailed consideration of the coherent fractions for the F absorption data, indicates a significant preference for a slight tilt of the molecular symmetry axis such that a molecular mirror plane is aligned in the ⟨0 1 1⟩ azimuth, with the two equivalent F atoms tilted down closer to the surface. The static tilt required to achieve this improved description of the NIXSW is only ~5–10°, well within the estimated precision of the NEXAFS result. Incorporating this static tilt also defines the azimuthal orientation of the PF_3 species as having their molecular mirror plane aligned in the ⟨0 1 1⟩ close-packed direction of the Cu(1 0 0) surface.

While at first sight the implied molecular tilt is surprising, and has certainly not been seen in any previous studies of adsorbed PF_3, inspection of Fig. 1 serves to remind us that introducing a threefold symmetric molecule onto a fourfold symmetric substrate leads to a system of much-reduced symmetry, with only a single mirror plane

remaining. This contrasts with all previous adsorption studies of PF_3 conducted on threefold symmetric substrates. Notice, too, that the plane in which the molecular tilt is proposed, the $\langle 0\,1\,1\rangle$ direction of the upper diagram of Fig. 1 (which shows the preferred azimuthal orientation of the molecules) corresponds to the direction of the closest intermolecular distances, a value less than the estimated van der Waals radii. It is thus only in this direction that the intermolecular interactions can prevent the free rotation of the adsorbed PF_3 species, and in the absence of such free rotation there is no static or time-averaged twofold rotational or mirror symmetry to preclude tilting. As such, there is no reason *not* to expect tilting in this direction.

There remains, however, one unexplained feature of the results presented here, namely the significant reduction of the projection of the P–F bond length along the molecular symmetry axis, implying a substantial increase in the F–P–F bond angles relative to the gas-phase species. In the gas-phase molecule it is known that the umbrella vibrational mode of the molecule is rather soft, so this distortion is unlikely to have a high energy cost, yet no such distortion appears to occur in the same species adsorbed on both Ni(1 1 1) and Cu(1 1 1). Two differences between the Cu(1 0 0) surface on the one hand, and the Ni(1 1 1) and Cu(1 1 1) surfaces on the other, could be relevant. One is that the rotational symmetry mismatch of the molecule and the surface on Cu(1 0 0) makes a solution with a tilted molecule more likely (and indeed, we find evidence for such a tilt) and this brings (two of) the F atoms closer to metal surface and thus more able to interact with it. The second is that the packing density of the molecules in the Cu(1 0 0)$c(4\times 2)$ phase is $\sim$15% lower than in the Ni(1 1 1)(2×2) surface, although the intermolecular distance is almost identical. This could mean that it is easier to accommodate the larger van der Waals radii of the distorted PF_3 molecules (with enlarged F–P–F angles) on the Cu(1 0 0) surface. Unfortunately, no ordered LEED pattern was seen in the Cu(1 1 1)/PF_3 system (perhaps due to enhanced electron-beam desorption cross-sections) so we can only surmise that saturation on this surface would also lead to a (2×2) ordering. However, neither of these differences between the (1 0 0) and (1 1 1) surfaces seems to offer a compelling reason for expecting the significant difference in F–P–F bond angles, and it would certainly be of interest to see if this difference is reproduced by modern total-energy calculations for these systems.

Acknowledgements

The authors are pleased to acknowledge the financial support of the Engineering and Physical Sciences Research Council in the form of a research grant including provision for access to the Daresbury Synchrotron Radiation Source. MSK acknowledges the support given by the King Fahd University of Petroleum and Minerals. Jane Hinch (Rutgers University) is thanked for providing information on the Cu(1 0 0)/PF_3 system prior to publication.

References

[1] F. Nitschké, G. Ertl, J. Küppers, J. Chem. Phys. 74 (1981) 5911.
[2] M.D. Alvey, J.T. Yates Jr., K.J. Uram, J. Chem. Phys. 87 (1987) 7221.
[3] M. Kerkar, D.P. Woodruff, J. Avila, M.C. Asensio, M. Fernandez-Garcia, J.C. Conesa, J. Phys.: Condens. Matter 4 (1992) 6509.
[4] R. Dippel, K.-U. Weiss, K.-M. Schindler, P. Gardner, V. Fritzsche, A.M. Bradshaw, M.C. Asensio, X.M. Hu, D.P. Woodruff, A.R. González-Elipe, Chem. Phys. Lett. 199 (1992) 625.
[5] S. Liang, M. Trenary, J. Chem. Phys. 89 (1988) 3323.
[6] N.J. Sack, T.E. Madey, Surf. Sci. 347 (1996) 367.
[7] R.G. Jones, N.E. Abrams, G.J. Jackson, N.A. Booth, M.T. Butterfield, B.C.C. Cowie, D.P. Woodruff, M.D. Crapper, Surf. Sci. 414 (1998) 396.
[8] J. Braun, G.G. Bishop, A.V. Ermakov, L.V. Goncharova, B.J. Hinch, J. Chem. Phys. 110 (1999) 5337.
[9] D.P. Woodruff, Prog. Surf. Sci. 57 (1998) 1.
[10] D.P. Woodruff, Rep. Prog. Phys. 68 (2005) 743.
[11] M.D. Alvey, J.T. Yates Jr., J. Am. Chem. Soc. 110 (1988) 1782.
[12] H.-S. Tao, U. Diebold, V. Chakarian, D.K. Shuh, J.A. Yarmoff, N.D. Shinn, T.E. Madey, J. Vac. Sci. Technol. A 13 (1995) 2553.
[13] K.-U. Weiss, R. Dippel, K.-M. Schindler, P. Gardner, V. Fritzsche, A.M. Bradshaw, D.P. Woodruff, M.C. Asensio, A.R. González-Elipe, Phys. Rev. Lett. 71 (1993) 581.
[14] S.A. Joyce, J.A. Yarmoff, T.E. Madey, Surf. Sci. 254 (1991) 144.
[15] G.J. Jackson, J. Lüdecke, D.P. Woodruff, A.S.Y. Chan, N.K. Singh, J. McCombie, R.G. Jones, B.C.C. Cowie, V. Formoso, Surf. Sci. 441 (1999) 515.
[16] S. Doniach, M. Sunjic, J. Phys. C: Solid State Phys. 3 (1970) 285.
[17] D.P. Woodruff, Rep. Prog. Phys. 49 (1986) 683.
[18] XSWfit is a procedure, written as an Igor-Pro macro, which automatically fits XSW data. It is based on the formalism originally developed by D.P. Woodruff in Fortran for calculating the XSW profile for a given set of parameters. A copy of the Igor routines can be obtained from Rob Jones, email: robert.g.jones@nottingham.ac.uk.
[19] J. Zegenhagen, Surf. Sci. Reports 18 (1993) 199.
[20] D.P. Woodruff, B.C.C. Cowie, A.R.H.F. Ettema, J. Phys.: Condens. Matter 6 (1994) 10633.
[21] J. Lee, C. Fisher, D.P. Woodruff, M.G. Roper, R.G. Jones, B.C.C. Cowie, Surf. Sci. 494 (2001) 166.